DOI: 10.13009/EUCASS2017-687

An Integrated Approach to Swept Wing Icing Simulation

Mark G. Potapczuk and Andy P. Broeren**
** NASA John H. Glenn Research Center*
Cleveland, Ohio, 44135 USA

Abstract

This paper describes the various elements of a simulation approach used to develop a database of ice shape geometries and the resulting aerodynamic performance data for a representative commercial transport wing model exposed to a variety of icing conditions. This effort included testing in the NASA Icing Research Tunnel, the Wichita State University Walter H. Beech Wind Tunnel, and the ONERA F1 Subsonic Wind Tunnel as well as the use of ice accretion codes, an inviscid design code, and computational fluid dynamics codes. Additionally, methods for capturing full three-dimensional ice shape geometries, geometry interpolation along the span of the wing, and creation of artificial ice shapes based upon that geometric data were developed for this effort. The icing conditions used for this effort were representative of actual ice shape encounter scenarios and run the gamut from ice roughness to full three-dimensional scalloped ice shapes. The effort is still underway so this paper is a status report of work accomplished to date and a description of the remaining elements of the effort.

1. Introduction

Simulation of an aircraft encounter with environmental icing conditions has been undertaken from the earliest years of flight in an effort to protect against this hazardous condition. Experimental simulation has been undertaken in icing wind tunnels, in climactic chambers, in engine test stands, and by flying behind an icing tanker aircraft. Computational simulation of icing encounters is a more recent approach and has been developed significantly over the past four decades. An evaluation of an icing encounter for a complete full-scale aircraft can be performed in one of two ways; actual flight into icing conditions or a full three-dimensional computational simulation. Flight testing is expensive, is dependent upon the availability of desired conditions, and can potentially be hazardous. Computational simulation of an aircraft encounter with icing holds promise for a more cost effective approach, however, there are still elements of icing physics required for accurate modelling that are not understood, as well as a lack of significant validation data for complete aircraft configurations. The method currently employed to simulate icing and its impact on an aircraft is typically a two-step process. The first step involves the use of aircraft component models tested in an icing wind tunnel at the desired icing conditions. This is followed up with construction of artificial reproductions of the resulting ice shapes which are attached to either the same model or an equivalent model designed for aerodynamic testing, and tested in an aerodynamic wind tunnel.

A multi-year effort is currently underway to create a publicly-available, high-quality, three–dimensional ice-accretion database and associated aerodynamic data to evaluate the performance of icing simulation tools for large-scale swept wings. This activity is a joint effort sponsored by the National Aeronautics and Space Administration (NASA), the Federal Aviation Administration (FAA) and the Office National d'Etudes et Recherches Aérospatiales (ONERA) with collaboration from the Universities of Illinois, Virginia, and Washington as well as with the Boeing Company. This research is an integrated approach employing icing tunnel testing, aerodynamic tunnel testing, icing scaling methods, and computational ice accretion codes as well as computational fluid dynamics codes. The combination of these tools was necessary to develop the resulting database of ice shapes and aerodynamic information in a manner that was consistent with the expected outcome for the complete wing in an actual icing encounter.

1.1 Motivation

Design considerations and certification of an aircraft for flight in icing conditions is a necessary but costly effort for any manufacturer. Flight safety is a critical element that is addressed in a conservative manner but can be made less costly by developing effective, accurate simulation methods as a substitute for flight testing. In order to determine how effective any simulation method must be in representing an actual icing encounter, criteria must be developed for assessment of such simulations. Such criteria are dependent upon the systems being simulated and the measure required to assess that system. Typically, the two major purposes for icing simulation are to assess the aerodynamic performance

DOI: 10.13009/EUCASS2017-687

of the vehicle with ice on the lifting surfaces and to determine the effectiveness of an ice protection system. In the latter case, a failed ice protection system and partial ice removal can result in ice remaining on the surface and again its aerodynamic effects become a measure of the effectiveness.

With assessment of aerodynamic performance losses due to ice accretion as a criterion for accurate simulation of an icing encounter, the question arises as to how much of the ice shape geometric detail must be reproduced to be assured of a reasonable simulation of an actual encounter. With that in mind, this research effort was designed to generate accurate ice shape geometries as well as lower fidelity representations of the same geometries and then determine the differences, if any, in the aerodynamic characteristics. An example of high and lower fidelity models for a representative ice shape on a 2D NACA 23012 airfoil are shown in Fig. 1.

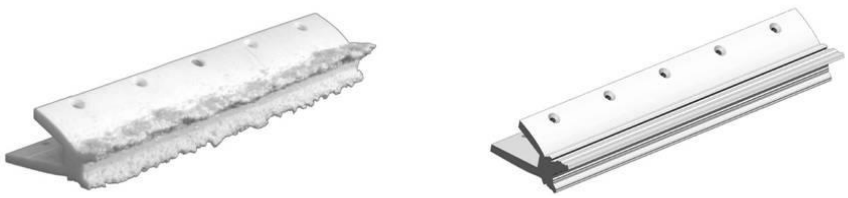

(a) (b)

Figure 1: High (a) and lower fidelity (b) models for the same ice shape

These shapes are used in an aerodynamic wind tunnel to measure the changes in performance characteristics, such as those shown in Fig. 2.

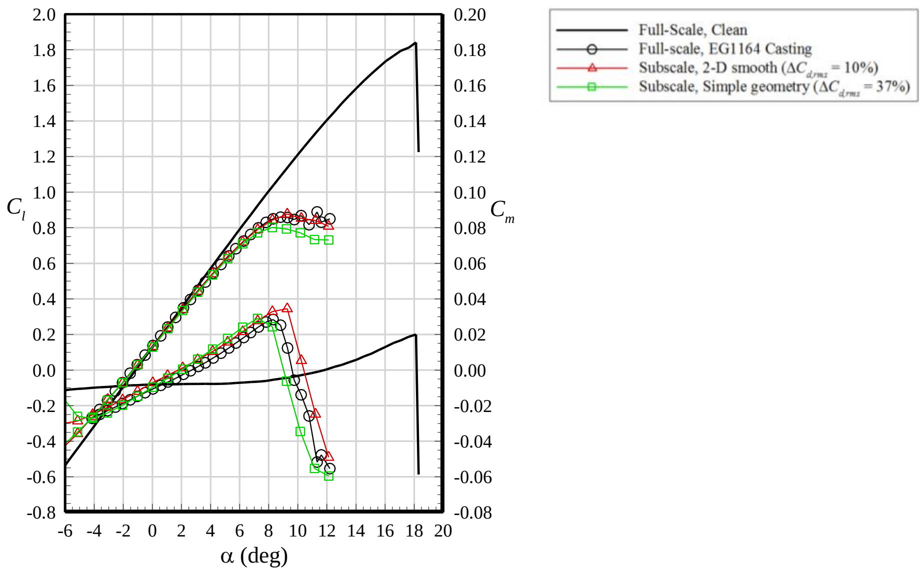

Figure 2: Changes to performance characteristics from leading edge ice accretions

The simulation of ice accretion and measurement of resulting aerodynamic performance changes has been conducted by numerous research organizations during the past few decades. Some notable work is that of Ingleman-Sundberg et al. [1], Bragg and Gregorek [2], Broeren et al. [3] and Addy [4]. Excellent summaries of the aerodynamic changes due to ice accretion and the experimental efforts that produced such data were presented by Lynch and Khodadoust [5] and Bragg et al. [6].

An earlier effort by NASA, ONERA, and the University of Illinois was conducted during the period of approximately 2004 to 2007. In that activity, designated as “SUNSET 1” [3] a two-dimensional NACA 23012 airfoil model was used to examine the influence of geometric fidelity on the performance characteristics associated with various categories of ice accretion. Small scale aerodynamic testing was performed in the University of Illinois subsonic wind tunnel on an 18-inch chord NACA 23012 model for a Reynolds number of 1.8×10^6 and a Mach number of 0.18. Ice shapes with similar geometric characteristics were also tested on a 72-inch chord version of that airfoil in the ONERA F1 wind tunnel over Reynolds numbers from 4.5×10^6 to 15.9×10^6 and Mach numbers from 0.10 to 0.28. Conclusions from that effort included the following. Geometric scaling of gross ice-shape features is appropriate for horn ice, streamwise ice,

DOI: 10.13009/EUCASS2017-687

and spanwise-ridge ice. For roughness and streamwise ice, the reproduction or simulation of small roughness features is important for accurate aerodynamic simulation.

The research effort being described in this report aims to extend the existing three-dimensional database by utilizing a wing that is representative of a modern commercial transport aircraft. The process undertaken to produce the ice shapes and subsequently test them in an aerodynamic wind tunnel required a well-integrated effort encompassing use of computational fluid dynamic (CFD) software, an ice accretion prediction code (LEWICE3D [7]), ice accretion testing in the NASA Icing Research Tunnel (IRT) [8], digital measurement of ice shape geometry [9], creation of model ice shapes of varying geometric fidelity [10], and aerodynamic testing in the Wichita State University Walter H. Beech Wind Tunnel [11] as well as in the ONERA F1 Pressurized Subsonic Wind Tunnel.

1.2 Objective and Approach

The objective of this research is to determine the necessary level of geometric fidelity required in a simulated ice shape to reproduce the aerodynamic characteristics of the highest fidelity version of a given ice shape. In order to achieve that objective, innovative methods for model development and testing were created and employed by the research team. As mentioned above, the effort consisted of many elements which were used in an integrated fashion to address the difficulties of testing a model representative of a commercial transport aircraft wing in facilities which require the use of scaled models. In addition to the normal issues of aerodynamic scaling, there are the inherent problems of creating a full span ice shape that is representative of what would develop on an actual wing and how to document and reproduce such ice shapes at levels of detail approaching that of the actual ice accretion.

The approach taken in this research was to connect everything back, as closely as possible, to conditions representative of an actual commercial transport aircraft in typical icing conditions. To do this, the first choice made by the team was to determine what geometry to use for the simulation. The selection process was complex given the large number of variables, such as sweep angle, aspect ratio, mean aerodynamic chord and wing span. An additional requirement was for all of the geometry to be nonproprietary and non-export controlled. After reviewing the available options, the Common Research Model geometry without the engine nacelle/pylon was selected [12].

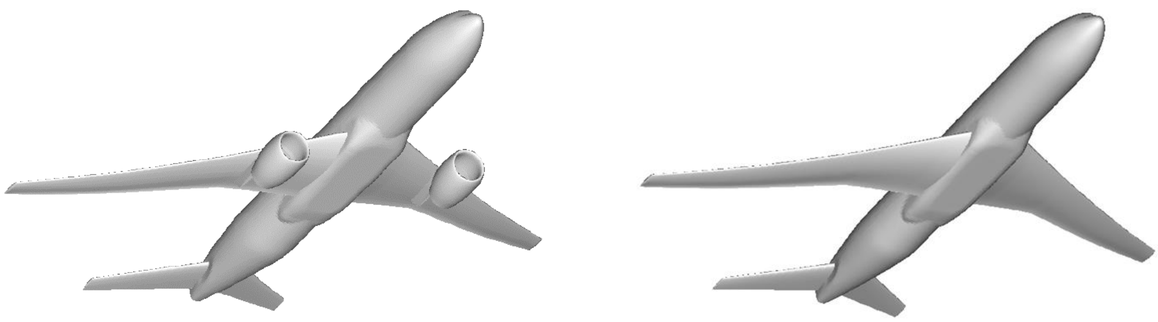

Figure 3. Conceptual design of the Common Research Model with and without engine nacelle/pylon.

Large-scale wing ice accretion testing requires the design of “hybrid” or “truncated” models where the full-scale leading edge geometry is matched to a shortened or truncated afterbody. The large physical size of the CRM wing requires a very aggressive design for the icing tunnel model that presents potential risk of adverse effects when installed in the NASA IRT. For aerodynamic wind tunnel testing, the full-scale CRM wing can be scaled to an appropriate size for the facility. In the case of the ONERA F1 wind tunnel, an 8 percent scale model of the CRM would be of appropriate size. While this is not unreasonable for the clean, baseline model geometry, such a large scale reduction becomes challenging when the goal is to accurately simulate ice accretion geometry that includes small roughness. Typical ice roughness sizes on the full-scale model ice accretion could be in the range of 0.04 to 0.08 in. (1 to 2 mm) which is equivalent to 0.003 to 0.006 in. (0.08 to 0.16 mm) on the 8 percent scale aerodynamic model. Small roughness features of this size are very challenging to accurately reproduce on the artificial ice shapes developed for aerodynamic testing. Based upon these factors, the research team decided to use a 65 percent scale version of the CRM as the full-scale, baseline, reference geometry for this research. Table 1 provides a comparison of the CRM65 geometry with that of existing single-aisle commercial transport airplanes.

Once the CRM65 wing was selected as the geometry to be used for this research, a series of analyses were required to properly size the models to be built for testing in the IRT and the two aerodynamic facilities. The process of performing

DOI: 10.13009/EUCASS2017-687

these computational analyses, the design of the models, the selection of the appropriate test conditions and the resulting testing in the selected facilities constitute the integrated icing simulation effort that is the subject of this report.

Table 1. Comparison of CRM65 wing geometry with existing single-aisle airplanes*

Airplane	Span (ft)	Mean aerodynamic chord (ft)	Area (ft^2)	Aspect ratio	Taper ratio	Sweep angle
CRM65	125.3	15.0	1.745	9.0	0.28	35°
Airbus A320	112.0	14.1	1.320	9.5	0.21	25°
Boeing 737-800	112.6	13.0	1.341	9.5	0.16	25°
Boeing 757-200	124.8	16.7	1.847	7.8	0.21	25°

* Data for existing single-aisle airplanes was compiled from publically-available sources that may use different conventions to define the geometric parameters.

2.0 Description of the Simulation Elements

The most realistic method for determining the impact of an icing encounter on an aircraft wing is to actually fly the aircraft through an actual icing cloud. In doing so, however, there are a number of drawbacks when it comes to actual measurements and documenting the encounter to the degree needed to extract useful information relative to the goals of this research. Some of those deficiencies include; non-constant icing conditions during the encounter, the inability to precisely measure the resulting ice shapes, and the fact that the impact of the ice accretion cannot be isolated to the wing alone. In order to overcome these drawbacks and to more easily obtain the necessary data for the objective of this research, ground-based testing is the only feasible method to be used. Since no icing facility available is large enough to encompass a full-scale commercial transport wing, sub-scale model testing is required. Likewise, aerodynamic testing of the CRM65 full span wing model also requires the use of sub-scale models.

Thus, the experimental simulation effort conducted for this research consists of testing wing section models in the NASA IRT and sub-scale wing models with artificial ice shapes in the WSU wind tunnel and the ONERA F1 wind tunnel. In order to conduct these experimental simulations, a series of computational simulations were also conducted, including ice accretion calculations for the actual CRM65 wing and the IRT wing section models, as well as, CFD analyses of the various models to be tested in the IRT and the wind tunnels. These simulation efforts were tied together through the geometry of the ice shapes themselves. In order to produce ice shapes that could be used in different sized models for two significantly different wind tunnel test sections a method of digitally recording 3D ice shape geometry, scaling it to different sized models, and producing accurate reproductions of the original shapes was developed. A more detailed description of these various elements of the integrated simulation method are described below and in the documents referenced therein.

2.1 Analysis of the Wing in Flight

The first step in determining what was to be simulated in this research effort was to select a set of icing conditions and to identify what ice accretions to expect on the full scale CRM65 wing. The conditions selected for analysis were representative of flight conditions for a commercial transport aircraft exposed to icing. Some examples of conditions used for this analysis are shown in Table 2. Analysis of the CRM65 was performed using the CFD software tool, OVERFLOW [13,14] and with the LEWICE3D ice accretion software. The CFD solutions for the clean geometry are designated the Clean Flight Baseline (CFB). These results were input to the LEWICE3D software to produce the Iced Flight Baseline (IFB).

Table 2. Representative flight conditions for an icing encounter simulation

Condition	Phase	Altitude (ft)	T_{amb} (°C)	M	α (deg)	LWC (g/m^3)	MVD (μm)	t (min)
WB52 T-25	Descent	5,000	-25	0.41	2.10	0.1700	20	4.1
WB33 T-6	Hold	10,000	-6	0.36	3.67	0.5090	20	45.0
WB39 T-20	Hold	22,000	-20	0.46	3.64	0.2100	20	45.0
WB41 T-13	Hold	5,000	-13	0.35	4.38	0.3605	20	45.0
WB47 T-6	Hold	15,000	-6	0.43	4.36	0.5090	20	45.0

A representative result is shown in Fig. 4 for flight condition WB33 T-6 at 10,000 ft altitude, speed = 232 kt, static temperature = –6 °C, airplane angle of attack = 3.7°, droplet MVD = 20 μm, cloud LWC = 0.5090 g/m^3 and an exposure time of 45 min. Fig. 4 depicts the LEWICE3D generated ice shapes at several locations along the span of the wing.

DOI: 10.13009/EUCASS2017-687

For this case, the predicted ice shape is a large upper-surface horn. Results of this type were generated for all of the icing cases selected for analysis.

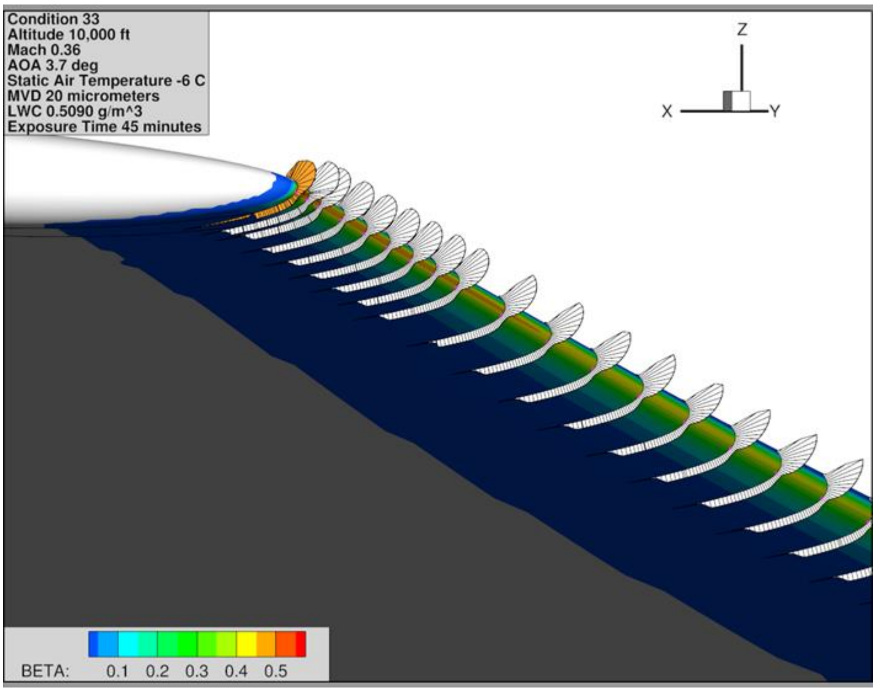

Figure 4. LEWICE3D ice shape results for CRM65, droplet MVD = 20μm, V = 232kt, altitude = 10,000ft, LWC = 0.5090g/m^3, static temperature = -6°C, 45-min exposure.

These results provide an anchor for the subsequent analysis. The results of the analysis for the hybrid models to be tested in the IRT should resemble the ice shapes from the Iced Flight Baseline analysis. Likewise, the ice shapes actually generated in the IRT should resemble those of the IFB.

2.2 Selection and Design of the Icing Wind Tunnel Models

The CRM65 wing dimensions are a span of 125.3 ft, a chord of 25.4 ft at the side of the body, and a chord of 5.82 ft at the wing tip. Thus, testing in the NASA IRT, with a 6 ft by 9 ft by 20 ft test section, precludes the use of a full-scale wing model. Use of a sub-scale full-span wing model in the IRT would require a scaling factor far beyond anything undertaken in existing scaling laws. It is also not clear that small scale ice structures, such as ice roughness and ice feathers can be scaled at all. As such, the approach taken in this research was to create models of discrete span-wise

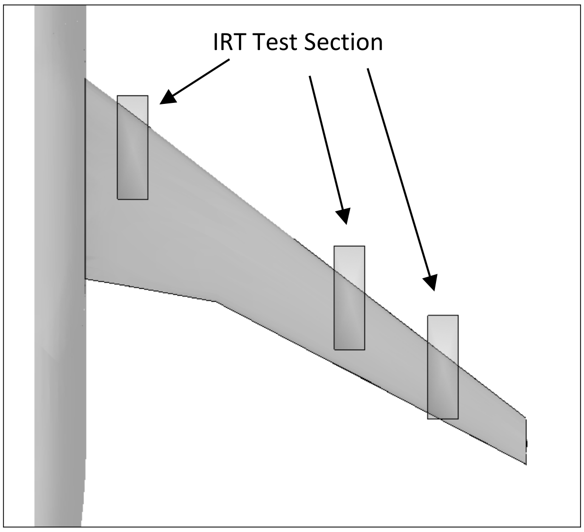

Figure 5. Full scale CRM65 wing overlaid with IRT test section planform outlines

sections of the wing at full scale dimensions, build ice at those locations, and develop a full-span model of the ice from that information. In doing so, three locations along the span of the wing were selected, one near the root of the wing, one at a mid-span location, and a third at a location near the tip of the wing. These selected locations are illustrated in Fig. 5 along with rectangular boxes identifying the plan-form dimensions of the IRT (9-ft. wide by 20-ft. long).

As illustrated in Fig. 5, even with discrete spanwise locations selected, full-scale models of the wing sections would still be longer than the entire length of the IRT test section. Thus, the use of truncated models based upon the work on hybrid airfoil models for ice accretion studies of Saeed et al. [15] was employed for this research. Extending that work to a swept wing configuration was a significant advancement in representing a large commercial transport wing geometry within the restricted confines of an icing wind tunnel. In using a hybrid wing section model, the idea is to retain the full scale geometry for the leading edge region within which the ice accretion limits are contained. The aft section of the model is then modified and designed to fit within the IRT test section and at the same time retain the correct flow and circulation for ice accretion on the full-scale leading edge. An example schematic of a hybrid airfoil is shown in Fig. 6.

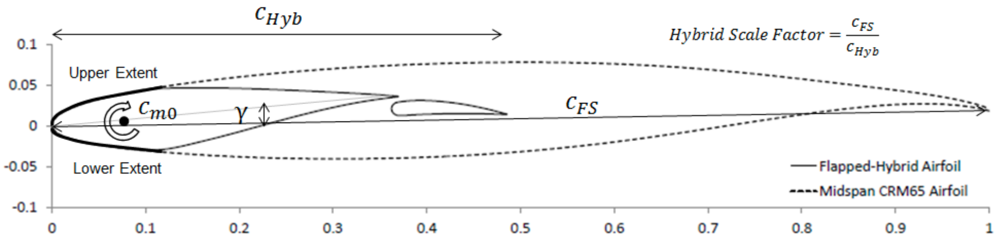

Figure 6. Flapped hybrid airfoil design schematic.

For this effort, the hybrid wing design for each selected spanwise station was performed in the following manner. A 2D hybrid airfoil model was designed using the methods described by Saeed et al. Although the CRM65 cruise wing was not designed with any high-lift devices, the hybrid model includes a flap in order to allow control of the flow thus enabling the desired reproduction of the flow at the leading edge. The hybrid airfoil coordinates were then extruded along a line perpendicular to the cross section. The geometry was then rotated to produce the desired sweep angle and the ends were cut off to fit within the height of the IRT (models are typically mounted vertically in order to minimize the solid and wake blockage). The model was then rotated to the desired angle of attack. CFD analysis of the model in the IRT was performed using FLUENT [16] with grid generation performed using Pointwise [17]. The flow simulations were run at varying angle of attack conditions and with varying flap deflections. These analyses were performed to match the attachment line location of the full-scale model at the desired run conditions.

The results were then examined to see if the following criteria were satisfied. Flow separation on the model was expected but should be within acceptable limits. The aerodynamic loads on the model had to be within tunnel safety limits. Spanwise flow variations should be limited, especially within the region approximately 12 inches above and below the centerline elevation of the test section. Also, the ice shapes calculated for the full scale and hybrid airfoil models were compared to the LEWICE3D calculation of the ice shape at the same spanwise location for the full CRM65 wing geometry, see Fig. 7. Final checks on the model configuration included a determination of the need for icing scaling, a re-check of model loads with the ice shapes, and a determination if there was margin in the flap deflection to allow for adjustment during testing.

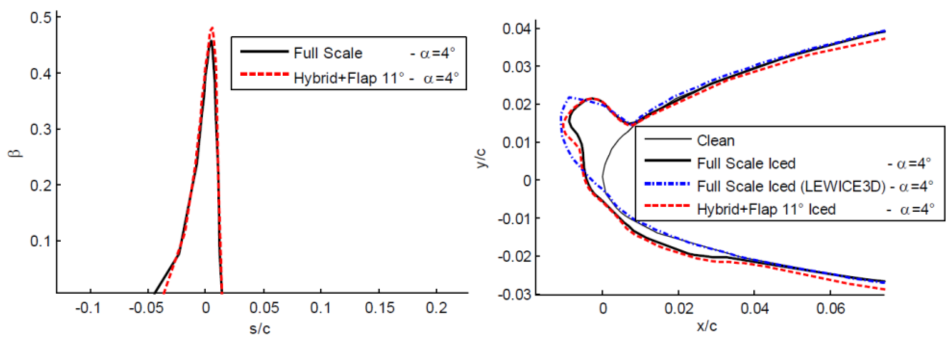

Figure 7. Comparison of full-scale and hybrid airfoil local collection efficiency and ice shape results for midspan station.

A much more thorough description of this process is found in the reports of Fujiwara et al. [18, 19].

DOI: 10.13009/EUCASS2017-687

2.3 Testing in the Icing Wind Tunnel

The models developed using the hybrid wing model methodology described in the previous section were fabricated and tested in a series of tests in the NASA IRT. The models were tested in three separate test campaigns. Each model was initially installed in the IRT test section with the pressure-instrumented leading edge. The model surface pressures were measured over a large range of angle of attack and flap deflections in order to track the location of the attachment line at the spanwise station 36 in. above the test-section floor (model centerline). At the conclusion of these aerodynamic tests, the pressure-instrumented leading edge was removed and the icing leading edge was installed. For icing tests, the desired temperature and speed conditions were established with the appropriate time allotted for the model and tunnel to thermally equilibrate. The icing spray cloud was turned on for the desired period of time and then the tunnel was shut down to allow for documentation of the ice accretion. Photographs were taken first, followed by 3-D digital measurement using a laser-based scanning system [9, 20, 21]. In some cases, a section of the ice was removed from the model and weighed after the 3-D measurements were completed.

The aerodynamic and icing test conditions were based upon the in-flight icing mission scenarios for the CRM65 airplane originally used in the hybrid model design process as described in Section 2.2. There were at least seven different mission scenarios that were considered during the model design phase. In planning for the IRT test campaigns, three of these scenarios were selected as the reference conditions. All of the cases are for the airplane operating in the cruise configuration which is consistent with the existing CRM65 geometry used for this work.

A key advantage and motivation behind the hybrid model design approach utilized in this effort was maintaining the full-scale wing leading-edge geometry in order to generate flight-scale representative ice accretion. However, the resulting model sizes were still large relative to the IRT test section. These large model sizes, particularly for the Inboard model, limited the maximum speed that could be obtained. This limitation was primarily due to the solid and wake blockage effects of the model in addition to high aerodynamic loads. Prior to the conduct of the testing, it was recognized that the selected speeds were most likely unrealistic, particularly for the Inboard model. Therefore, this model was tested in the first campaign and it was found that the optimum speed for icing tests was 130 knots for each case. It was determined that some margin on fan power was required and that running all three cases at the same speed was a useful simplification. Since a key objective of this work was to simulate the ice accretion that would build up on the CRM65 airplane wing, identical icing conditions including the speed of 130 knots were used for all three models. A limited set of conditions at higher speeds were also performed for the Midspan and Outboard models since these models could achieve such speeds.

The reference cases examined along with the speed limitation of 130 knots required modifications to the aerodynamic and icing conditions for the IRT tests. Further simplifications to the matrix were also performed in order to generate ice accretion that was more readily suited to icing-code evaluation. While this is appropriate for airplane certification icing analysis, the changes to multiple variables complicated the use of the resulting ice accretion for icing code evaluation. It was considered more useful to hold constant all other variables and vary the temperature over a desired range. Therefore, most of the IRT test conditions depart from the App. C envelope used for icing certification. In order to account for the reduction in speed to 130 knots, a scaling analysis was performed to match the freezing fraction at the attachment point and the product of the local collection efficiency at the attachment point and the accumulation parameter. These are standard scaling methods that have been developed primarily for model-size scaling applications [22].

2.4 Creation of the Artificial Ice Shapes

The ice shapes to be tested in the aerodynamic wind tunnels are meant to cover the entire span of the CRM65 wing model. From Sections 2.2 and 2.3 it is apparent that the ice shapes produced from the IRT testing only cover a small percentage of the span. In order to develop an ice shape that covers the entire span, a method for extending the existing data between the spanwise stations and beyond the inboard and outboard stations was devised. The concept is essentially a gradual transformation from one profile to another using the capabilities of the software used to post-process the data from the scanning procedure.

The method devised to generate full-span ice shapes involved interpolating between the scanned sections of the Inboard, Midspan, and Outboard CRM65 model ice shapes using the weighted averaging function in Geomagic Studio [23]. This is the same commercially available software that was used to scan the ice accretions and generate a water-tight surface mesh, which is a mesh that includes all complete surfaces and connects all surfaces without any discontinuities. It is important to point out that the 1-g cruise condition loading on the CRM65 wing was removed for simplicity. This resulted in a straight leading edge along the span of the wing model without any shear, allowing for much simpler interpolation of the ice shape.

DOI: 10.13009/EUCASS2017-687

A method was also devised to extrapolate ice shapes at the root and tip stations using the Inboard and Outboard model station ice shapes, respectively. LEWICE3D results were available for a limited set of icing conditions, but not at conditions identical to the experimental ice accretions. These results were used as an approximate guide to extrapolate the root and tip ice shapes.

Full details of the interpolation and extrapolation processes are described by Camello et al. [10]. A full-span high-fidelity ice shape resulting from this process is shown in Fig. 8.

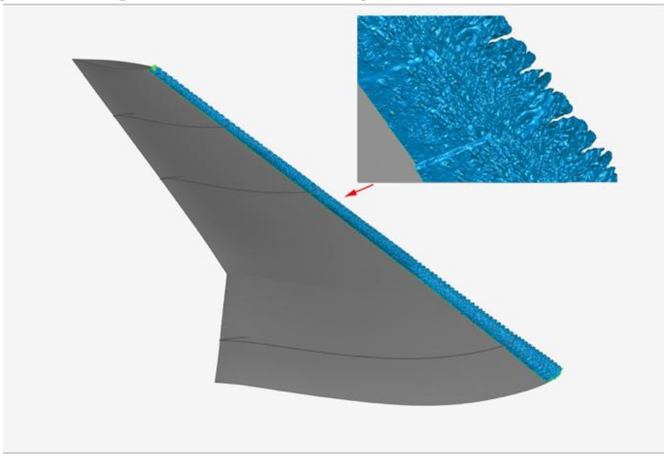

Figure 8. Ice shape segments combined into continuous shape on the CRM65 wing.

In addition to the high-fidelity artificial ice shapes, lower-fidelity models were developed. These of course are being used to better understand the impact of aerodynamic differences that arise from the decrease in fidelity. The reduced fidelity ice shapes are ice shape models that do not maintain the highly detailed, 3D characteristics and roughness of the original ice accretion. An example of a low-fidelity version of a high-fidelity ice shape is shown in Fig. 9. In addition to examining this effect experimentally, developing a better understanding of the importance of reproducing various geometric features in a computational simulation of an ice accretion is necessary to determine how much additional research is needed in that field.

There are two main approaches to lower fidelity versions of ice shapes used in this research. One method is to sample the high fidelity ice shape at various points along the span and create two-dimensional representations at those points. Then the two-dimensional cuts are lofted to create a continuous ice shape across the span. The second method is to use the two-dimensional cuts produced by a LEWICE3D simulation of the ice accretion and loft between those cuts to generate a full-span ice shape. These approaches create smoother versions of the high-fidelity shapes and, as seen in Fig. 9, in the case of scalloped ice shapes fill in the gaps between the large ice structures of those class of ice accretions. Finally, these smooth, lower-fidelity ice shapes can also be coated with grit to simulate rough surfaces while still maintaining the less detailed large scale structures.

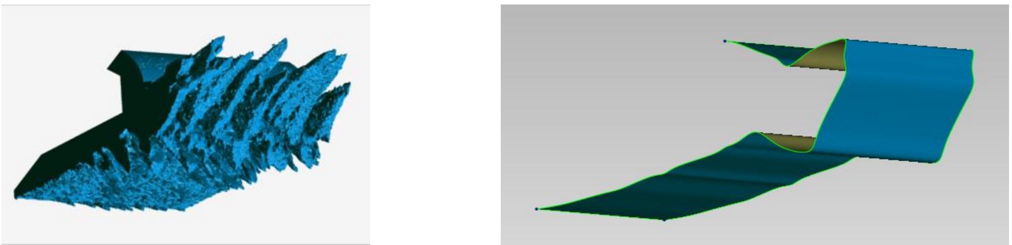

Figure 9. High fidelity ice shape from laser scan data compared to reduced fidelity version.

The artificial ice shapes created from these geometries, both high and low fidelity, are 3D printed using a stereolithography (SLA) rapid prototype manufacturing technique using the Somos® NeXt [24] material. The resulting ice shapes are then fitted with pressure taps in order to obtain pressure profiles for the entire iced wing at selected spanwise locations. These ice shapes are created in two or three spanwise segments, depending upon whether they are being used in the WSU tunnel or the ONERA F1 tunnel, and are fitted to specially designed aluminum elements. These artificial ice shapes and aluminum elements together constitute a removable leading edge structure that is mounted to the main body of the wing model, replacing an all-aluminum clean leading edge section. Full details of the artificial ice shape leading edge creation and fabrication are found in the report by Camello et al. [10].

DOI: 10.13009/EUCASS2017-687

2.5 Testing in the Aerodynamic Wind Tunnels

The final element of the integrated simulation effort is testing of the wing with multiple artificial ice shape leading edge configurations in an aerodynamic wind tunnel. As mentioned, aerodynamic testing occurred in two separate facilities, the WSU wind tunnel and the ONERA F1 pressurized wind tunnel. This enabled testing at two different geometric scales and at two Reynolds number ranges. The reason for testing at both facilities is to use the F1 tunnel to serve as a reference at higher Reynolds number conditions, closer to actual flight Reynolds numbers, and to compare those results to data from the lower Reynolds number WSU tunnel. The desired outcome is to be able to understand enough about any differences to be able to confidently use a smaller tunnel which enables a larger set of parametric studies both for financial and scheduling reasons.

Using the methodology described in the previous section, full-span ice shape models were built along with the main body of the CRM65 wing at the scales appropriate for use in the two wind tunnels. The wing model used in the WSU wind tunnel is an 8.9% scale version of the CRM65 wing and the model used in the ONERA F1 wind tunnel is a 13.3% scale version of that wing. The WSU wind tunnel is an atmospheric, closed-return type, subsonic wind tunnel with a 7 ft x 10 ft test section. The maximum speed of the tunnel is approximately 350 ft/s which corresponds to a Reynolds number per foot of approximately 1.8×10^6 and a maximum dynamic pressure of 125 psf. The ONERA F1 facility is an 11.4-ft x 14.8-ft pressurized wind tunnel. The pressurization capability of this facility allows for independent variations in Reynolds number up to approximately 12×10^6 and Mach number up to approximately 0.36. The results from the ONERA F1 test campaigns will be analyzed for Reynolds and Mach number effects (among other things) and compared to the results of the WSU test campaigns to determine the extent to which iced, swept-wing aerodynamic testing can be conducted in smaller-scale facilities at lower Reynolds number.

The CRM65 wing models with clean, high-fidelity ice shape, and low-fidelity ice shape leading edges were installed using splitter plates in each facility. Fig. 10 shows the 8.9% wing model with an artificial ice shape on the leading edge as mounted in the WSU tunnel. The models are equipped with rows of pressure taps and mounted on force balances. Tufts were applied to each model for flow visualization purposes. Additionally, in the WSU tunnel a wake survey system was used to better understand the structure of the flow aft of the iced wing as well as to provide spanwise distributions of lift and drag. Finally, oil flow visualization methods were used to obtain insight into the flow on the surface of the wing and how it is affected by the presence of the ice shape at the leading edge.

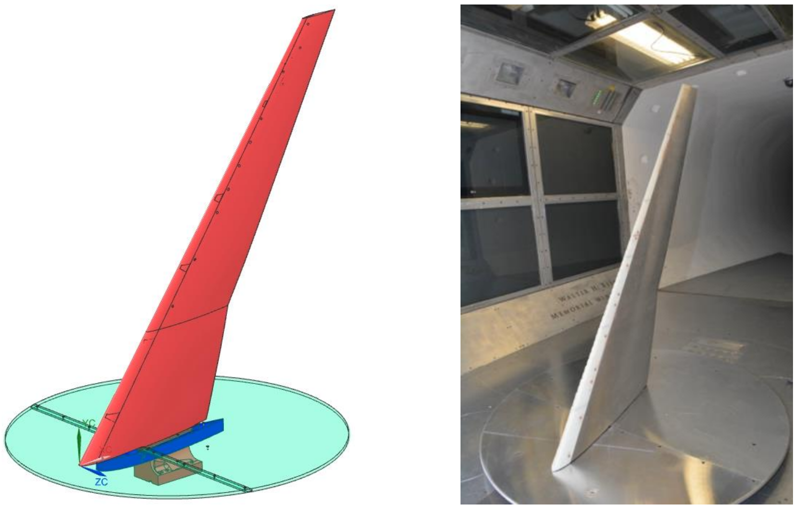

Figure 10. The WSU model is an 8.9% version of the CRM65 wing. CAD rendering and the model installed with a leading edge ice shape in the WSU tunnel.

More details of the WSU model can be found in the paper by Broeren, et al. [25]. Details regarding testing procedures at the WSU wind tunnel can be found in the papers by Camello, et al. [26] and Lum et al. [27]. Testing in the ONERA F1 facility with the 13.3% version of the CRM65 wing with similar artificial ice shapes was just completed at the time of publication for this report.

3.0 Results to Date

As seen from the description above, development of a simulation approach for ice growth and its aerodynamic effects on a realistic model representing a commercial transport wing is a multi-faceted activity. Several elements of this research have not been undertaken before and required the creation of novel new methods. This has resulted in a research effort that has spanned several years and engaged the expertise of several organizations. Thus, not all elements

DOI: 10.13009/EUCASS2017-687

of the effort have been completed to date. This section will summarize some of the results from the experimental and computational efforts that have been completed and reported on as of this publication. Full details of which can be found in the reports cited.

3.1 Ice Shape Database

As described above, the ice shapes generated for the Inboard, Midspan, and Outboard models were obtained during three separate test campaigns. The database generated from these tests includes photographs, 3D scans of the ice shapes, and in some cases the mass of ice for a designated spanwise length of the model. Details of the test results are found in the reports by Fujiwara, et al. [28] and Broeren, et al. [29].

The ice shapes generated in the IRT are used for a number of purposes. As described in Section 2.4, one of the uses is to form the basis for creating full span ice shape simulations. Another use of the ice shape data is to provide validation data for ice accretion codes. Since even three-dimensional ice accretion codes typically cannot, at this time, reproduce the scalloped ice shape features found from some swept wing ice accretions, a method of representing the scanned ice shapes as two-dimensional profiles was devised. This process of extracting 2D cuts out of the digitized ice shape is shown in Fig. 11 from Fujiwara et al. [30], where 30 cuts perpendicular to the model leading edge, 0.2 inch apart, were extracted and plotted in two dimensions. Then the outer boundary that leads to the Maximum Combined Cross Section (MCCS) of the ice sections was obtained for comparison to the computational simulations, giving a conservative (large) shape that was deemed closest to hand tracing. Details of this procedure are found in the report of Broeren et al. [29].

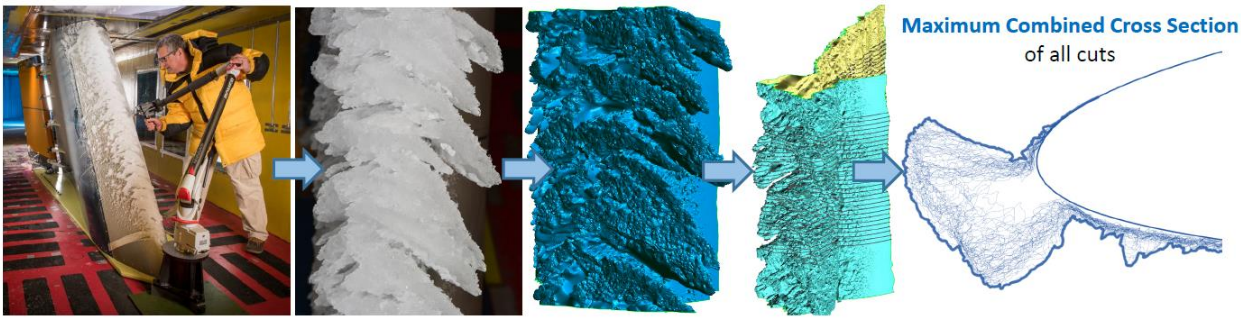

Figure 11. Extraction of 2D cuts from digitized scan of experimental ice shape.

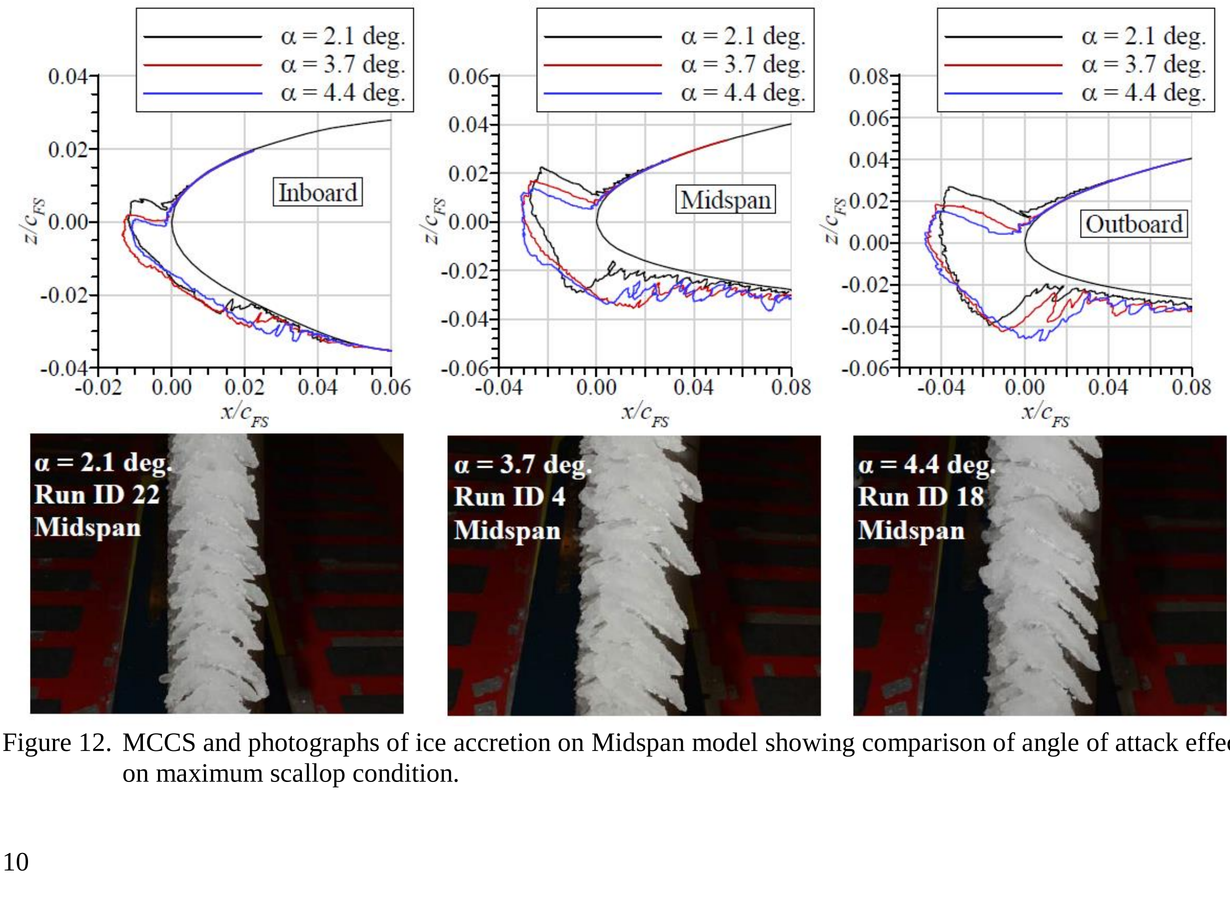

Figure 12. MCCS and photographs of ice accretion on Midspan model showing comparison of angle of attack effects on maximum scallop condition.

DOI: 10.13009/EUCASS2017-687

This series of ice-accretion tests was conducted for each model over a range of total temperatures from -23.8 °C to -1.4 °C with all other conditions held constant. The results showed the changing ice-accretion morphology from rime ice at the colder temperatures to highly 3D scallop ice in the range of -11.2 °C to -6.3 °C. Warmer temperatures generated highly 3-D ice accretion with glaze ice characteristics. The "maximum scallop" condition was associated with total temperature of -6.3 °C due to the large cross-section and large gaps between scallop features. The results indicated that the general ice morphology in terms of scallop features was similar for all three models. The location of the main ice shape was different for each model due to the local aerodynamic angle of attack. Since the Inboard model had the highest local angle of attack, the main ice shape was located on the lower-surface side of the leading edge hilite, whereas for the Midspan and Outboard models the main ice shape was located much closer to the hilite. Similar values of the dimensional maximum ice thickness were recorded for each wing section. Icing results were documented for limited parametric variations in angle of attack, drop size and cloud LWC. The effect of velocity on ice accretion was documented for the Midspan and Outboard models for a limited number of test cases. The data suggest that there are morphological characteristics of glaze and scallop ice accretion on these swept-wing models that are dependent upon the velocity. An example of the variation of ice shape as a function of angle of attack is shown in Fig. 12.

The ice shape data was used to examine the ability of LEWICE3D to simulate ice growth for these complex geometries. Comparisons have been made for complete scallops, incomplete scallops, and rime ice conditions as described by Fujiwara et al. [28]. An example of these comparisons is shown in Fig. 13, which also includes photographs of the ice shapes for reference purposes. The ice density value of 450 kg/m^3 is a value used to account for the gaps in scalloped ice shapes and is approximately one-third the value of solid ice. Results indicate that the LEWICE3D simulation has reasonable comparison to the MCCS profile for the Midspan and Outboard models. The LEWICE3D simulation is not as good for the Inboard model. Similar results were found for other test conditions leading to some need for examination of why the simulation did not perform as well for the large leading edge radius of the Inboard model.

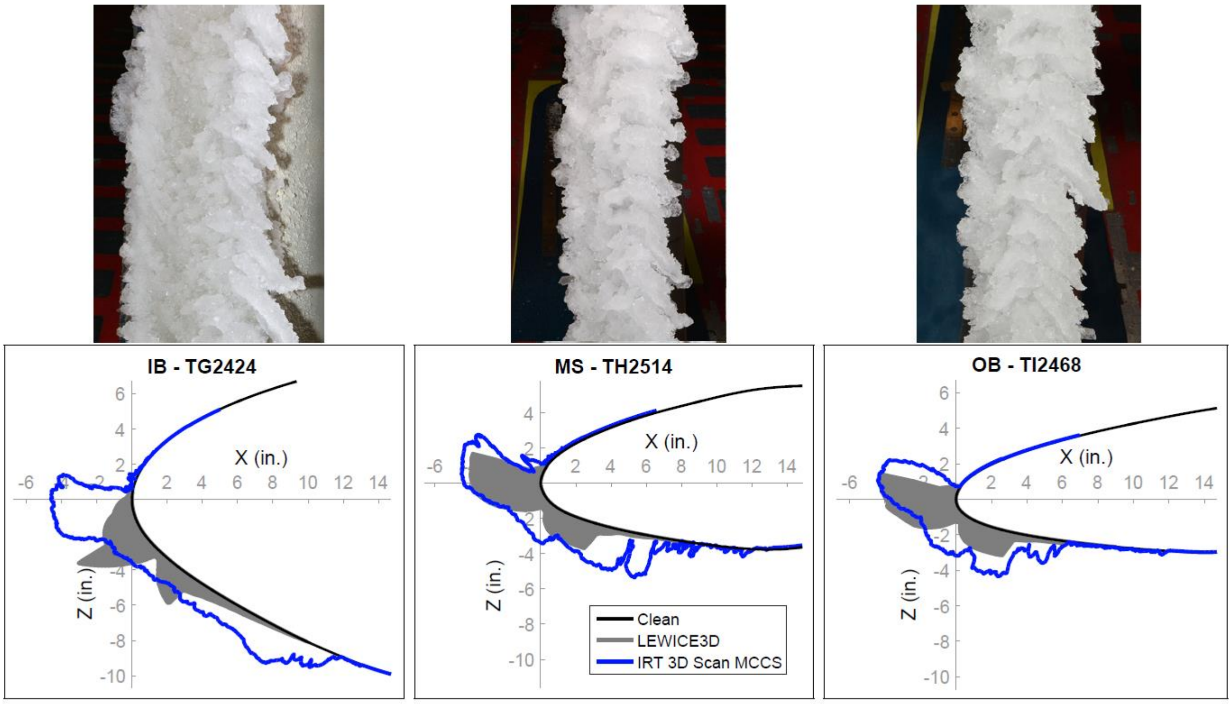

(a) Inboard model run TG2424. (b) Midspan model run TH2414. (c) Outboard model run TI2468.

Figure 13. WB33 icing condition. Comparison of MCCS profile to LEWICE3D with ice density = 450 kg/m^3.

3.2 Low Reynolds Number Aerodynamic Database

The aerodynamic testing in the WSU wind tunnel produced a significant data set for the clean and iced 8.9% CRM65 wing model. The data measured included pressures on the surface (including on the artificial ice shape surfaces), force balance measurements and five-hole probe wake survey measurements. Additionally, mini-tufts were placed on the surface of the wing and in separate runs surface oil flow visualization was performed. Computational fluid dynamics simulation of the clean wing performance was also conducted. CFD results for the ice wing performance changes have not been completed as of the date of this report but are being planned for future work.

DOI: 10.13009/EUCASS2017-687

In an initial campaign, prior to the IRT testing, the CRM65 wing was tested in a clean configuration, with an artificial ice shape based on a LEWICE3D ice accretion analysis, and with a leading edge geometry consisting of hemispherical bumps to simulate roughness. This test campaign was performed to obtain experience with the wing model and several interchangeable leading edge devices as well as to get some preliminary information on what to expect from the later artificial ice shape testing. This work is detailed in the report by Broeren, et al. [25]. It should be noted that the wake survey method was not employed during this initial campaign.

Following the NASA IRT test campaigns, artificial ice shapes were produced using the methods described in Section 2.4. These ice shapes were then tested, along with the clean wing configuration, in a later test campaign in the WSU wind tunnel. Results documented the performance losses for the various ice shape configurations tested. Fig. 14 shows a sample of the changes to force coefficients resulting from the maximum scallop ice shape configuration. Results from this test campaign are documented in the reports by Camello et al. [26] and Lum et al.[27].

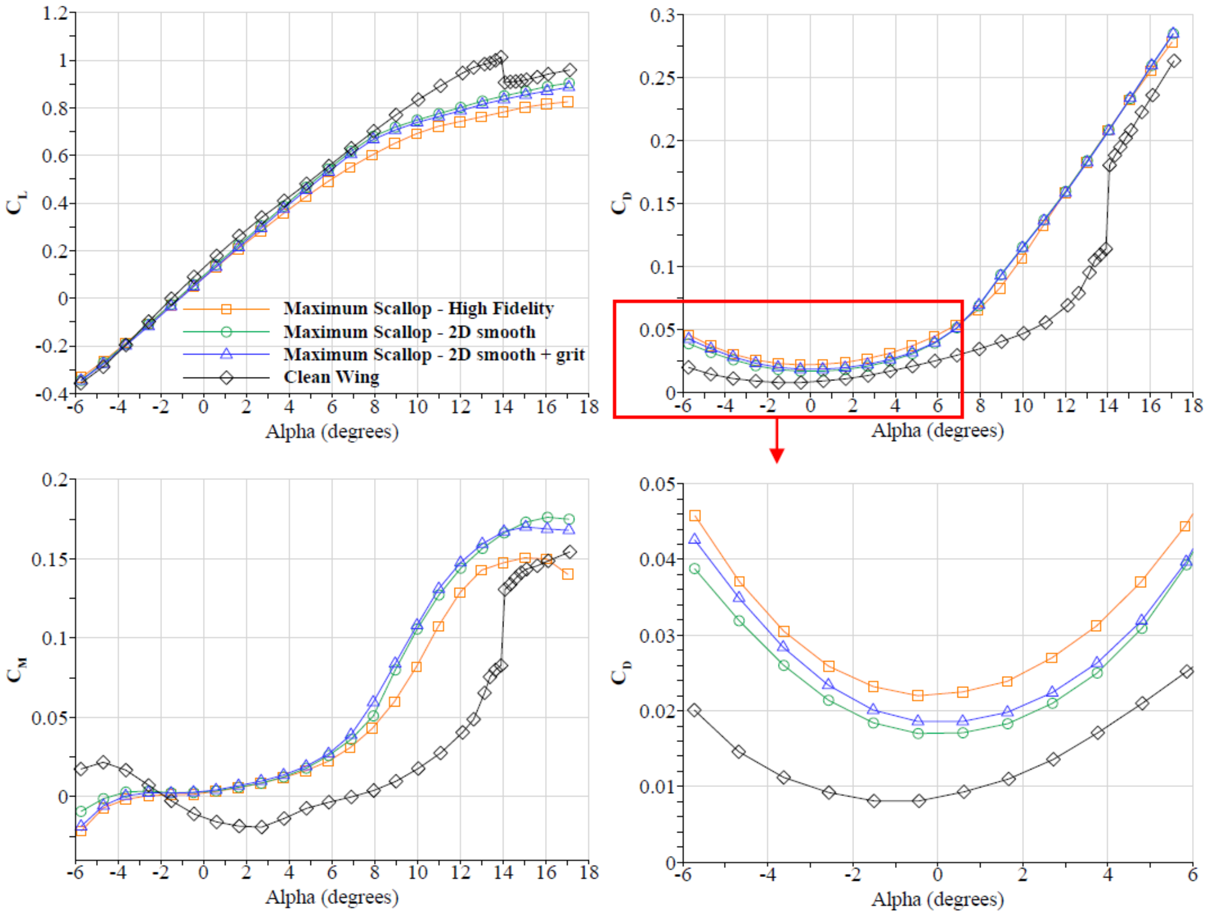

Figure 14. Force balance data for the 2D smooth, 2D smooth + grit, high-fidelity maximum scallop, and clean wing configurations for Re = 1.6 x 10^6 and M = 0.18.

Some of the conclusions from this test campaign include the following. Adding surface roughness to the 2D smooth streamwise ice shape produced force balance data similar to the high-fidelity streamwise ice shape force balance data. The 2D smooth and 2D smooth + grit maximum scallop configurations produced a higher amount of lift compared to the high-fidelity maximum scallop configuration, especially at higher angles of attack. Additionally, some results from the wake survey study include the following. Differences in lift measurements between the wake survey and the force balance ranged from 0.8% to 8.6%. Differences in drag measurements between the wake survey and the force balance ranged from 3.2% to 21%. The spanwise distributions for sectional profile and induced drag coefficients seemed to show a reaction to apparent streamwise vortices generated as a result of the maximum scallop ice shape. Individual vortices did not seem to appear in the spanwise calculations, possibly due to vortex interaction causing multiple streamwise vortices to coalesce. However, the wake survey was fairly coarse, and coalescence of the small vortices into larger ones could also be attributed to aliasing.

DOI: 10.13009/EUCASS2017-687

3.3 High Reynolds Number Aerodynamic Database

The aerodynamic test campaign in the ONERA F1 facility was just completed at the time of publication of this report. This campaign was conducted with the 13.3% model of the CRM65 wing with some of the same ice shapes that were tested in the WSU wind tunnel. One of the advantages of the 3D scanning method for ice shape documentation and the 3D printing method used for ice shape manufacturing is the ability to create the exact same geometry at different scale values. Preliminary results indicate similar trends to what was found in the low Reynolds number testing at WSU, however detailed analysis of the results will be required before any reporting and conclusions can be drawn.

4.0 Concluding Remarks

A highly integrated methodology for simulation of ice growth and resulting aerodynamic changes applied to a representative commercial transport wing has been developed. This approach to icing analysis employed all the current capabilities for ice accretion testing, computational simulation of ice accretion and aerodynamics, icing scaling methods, and aerodynamic wind tunnel testing for iced wings. Additionally, new methods have been developed to document ice shape geometries, create artificial ice shape models for full span wing models, extend hybrid airfoil design techniques to complete wing configurations, and to test large scale swept wing geometries in icing wind tunnels.

Some findings to date for this research effort include:

- Hybrid wing models can be developed to enable ice accretion testing on large scale wing leading edge geometries.
- A method has been created to document highly detailed three-dimensional ice shape geometries.
- A method has been created to extend the actual measured geometries to other spanwise locations across a wing model and produce realistic representations of an iced wing configuration.
- Icing condition scaling methods developed for straight and swept wing geometries are critical tools to aid in test matrix development for large scale models.
- CFD analysis of wings and wing sections both with and without tunnel walls are critical elements to enable the design of large scale models to be tested in the IRT which will accurately represent the icing environment for such models.
- Computational ice accretion simulation of complete wings and associated icing tunnel wing section models is a critical element for creation of such models.
- Comparison of the highly complex ice shapes generated on a swept wing model to ice shapes generated in an ice accretion code, no matter how realistic such computational results might be, is a difficult activity. New methods for making such comparisons are required for assessment of the computational tools.
- Aerodynamic data indicates that for large ice shapes, there is very little to no influence of Reynolds and Mach number on lift, drag, and pitching moment over the range tested for this cruise-wing configuration. For smaller ice shapes, such as rime ice geometries, there can be a difference in drag results as a function of Reynolds number. There are definitely differences due to Reynolds and Mach number for clean airfoil configurations and so assessing performance losses at different Reynolds and Mach numbers must be done with that result in mind.
- There are differences in performance characteristics between high fidelity and low fidelity ice shapes. 2D smooth configurations can be made to more closely match high fidelity aerodynamic results with the addition of grit to the 2D smooth configuration.

Additional insights from this work will be obtained from the current set of high Reynolds number tests in the ONERA F1 facility. Based on the testing results to date, an additional test campaign in the WSU wind tunnel will take place. Those results will then be used to plan a final test campaign in the F1 facility.

Acknowledgements

This report is a summary of a large body of work that has been conducted over the past few years. As such, the data and commentary for this report has been taken from many of the reports cited by the authors. In many cases, it was best to use the original author’s words directly rather than to reinterpret their work. Thus, the authors would like to acknowledge the work of the following individuals since their efforts constituted the research contained in this report. The research team consisted of Sam Lee, Brian Woodard, Mike Bragg, Chris Lum, Gustavo Fujiwara, Stephanie Camello, Adam Malone, Ben Paul, Yorum Yadlin, Brock Wiberg, Jeff Diebold, Chris Triphahn, Andrew Mortonson, Eric Loth, Chao Qin, Philippe Villedieu, Emmanuel Radenac, Frédéric Moens, Navdeep Sandhu, Jaime Katzer and Kevin Ho.

The authors would also like to thank the staffs of the Walter S. Beech Wind Tunnel at Wichita State University, the ONERA F1 Pressurized Wind Tunnel at Fauga-Mauzac, and the NASA Icing Research Tunnel in Cleveland. Their expertise was and is critical to the success of this research.

The authors would like to thank Quentin Schwinn and Jordan Salkin of Alcyon Technical Services (ATS) JV, LLC for their invaluable support in ice shape scanning and post-processing.

Finally, the authors would like to thank Jim Riley, Tim Smith, and Tom Bond of the FAA for their support and expertise.

This research was enabled by the support provided by NASA, FAA, and ONERA.

References

[1] Ingleman-Sundberg, M., O. Trunov, and A. Ivaniko. 1977. Methods for prediction of the influence of ice on aircraft flying characteristics. Report JR-1, a joint report from the Swedish-Soviet Working Group on Flight Safety.

[2] Bragg M., and G. Gregorek. 1982. Aerodynamic characteristics of airfoils with ice accretions. In: *AIAA 20th Aerospace Sciences Meeting*. AIAA-82-0282.

[3] Broeren, A., H. Addy Jr., M. Bragg, G. Busch, D. Guffond, and E. Montreuil. 2011. Aerodynamic simulation of ice accretion on airfoils, NASA/TP—2011-216929.

[4] Addy, H.E., Jr. 2000. Ice accretions and icing effects for modern airfoils. NASA/TP-2000-210031, April 2000; also U.S. Dept. of Transportation/Federal Aviation Administration Rept. DOT/FAA AR-99/89.

[5] Lynch, F. and A. Khodadoust. 2001. Effects of ice accretions on aircraft aerodynamics. *Progress in Aerospace Sciences*. Vol. 37, No. 8, pp. 669-767.

[6] Bragg, M., A. Broeren, and L. Blumenthal. 2005. Iced-airfoil aerodynamics, *Progress in Aerospace Sciences*. Vol. 41, No. 5, pp. 323-418.

[7] Bidwell, C., D. Pinella, and P. Garrison. 1999. Ice accretion calculations for a commercial transport using the LEWICE3D, ICEGRID3D and CMARC programs. NASA/TM-1999-208895

[8] Broeren, A., M. Potapczuk, S. Lee, A. Malone, B. Paul Jr., and B. Woodard. 2016. Ice-accretion test results for three large-scale swept-wing models in the NASA Icing Research Tunnel. NASA/TM—2016-219137. AIAA–2016–3733.

[9] Lee, S., A. Broeren, H. Addy Jr., R. Sills, and E. Pifer. 2012. Development of 3D ice accretion measurement method. In: *4th AIAA Atmospheric and Space Environments Conference*. AIAA-2012-2938.

[10] Camello, S., S. Lee, C. Lum, and M. Bragg. 2016. Generation of fullspan leading-edge 3D ice shapes for swept-wing aerodynamic testing. In: *8th AIAA Atmospheric and Space Environments Conference*. AIAA-2016-3737.

[11] Broeren, A., B. Woodard, J. Diebold, and F. Moens. 2017. Low-Reynolds number aerodynamics of an 8.9% scale semispan swept wing for assessment of icing effects. In: *9th AIAA Atmospheric and Space Environments Conference*. AIAA-2017-4372.

[12] Vassberg, J., M. DeHann, S. Rivers, and R. Wahls. 2008. Development of a Common Research Model for applied CFD validation studies. In: *26th AIAA Applied Aerodynamics Conference*. AIAA-2008-6919.

[13] Robinson, B., A. Verhoff, and W. LaBozzetta. 1994. Preliminary findings in certification of OVERFLOW. In: *25th AIAA Fluid Dynamics and Co-located Conferences*. AIAA-94-2236.

[14] Jespersen, D., T. Pulliam, and P. Buning. 1997. Recent enhancements to OVERFLOW," In: *25th AIAA Aerospace Sciences Meeting & Exhibit*, AIAA-97-0644.

[15] Saeed, F., M. Selig, and M. Bragg. 1997. Design of subscale airfoils with full-scale leading-edges for ice accretion testing. *AIAA Journal of Aircraft*. Vol. 34, No. 1, pp. 94-100.

[16] ANSYS FLUENT 12.0 User's Guide. 2009. ANSYS, Inc.

[17] Pointwise User Manual. 2013. Pointwise, Inc. pp. 306-318.

[18] Fujiwara, G., B. Woodard, B. Wiberg, A. Mortonson, and M. Bragg. 2013. A hybrid airfoil design method for icing wind tunnel tests. *Fluid Dynamics and Co-located Conferences, American Institute of Aeronautics and Astronautics*. AIAA-2013-2826.

[19] Fujiwara, G., B.Wiberg, B. Woodard, B., and M. Bragg.2014. 3D swept hybrid wing design method for icing wind tunnel tests. In: *6th AIAA Atmospheric and Space Environments Conference*. AIAA-2014-2616.

DOI: 10.13009/EUCASS2017-687

[20] Lee, S., A. Broeren, R. Kreeger, M. Potapczuk, and L. Utt. 2014. Implementation and validation of 3-D ice accretion measurement methodology. In: *6th AIAA Atmospheric and Space Environments Conference*. AIAA-2014-2613.

[21] Broeren, A.P., H. Addy, Jr., S. Lee, and M. Monastero. 2015. Validation of 3-D ice accretion measurement methodology for experimental aerodynamic simulation. NASA TM-2015- 218724.

[22] Anderson, D. 2004. Manual of scaling methods. NASA CR-2004-212875.

[23] 3D scanning, design and reverse engineering software from 3D systems. 2016. Geomagic. URL: http://www.geomagic.com

[24] Product Data Sheet: Somos® NeXt. 2016. Somos®, URL: https://www.dsm.com/

[25] Broeren, A., B. Woodard, J. Diebold, and F. Moens. 2017. Low-Reynolds number aerodynamics of an 8.9% wing for assessment of icing effects. In: *9th AIAA Atmospheric and Space Environments Conference*. AIAA-2017-4372.

[26] Camello, S., M. Bragg, A. Broeren, C. Lum, B. Woodard, and S. Lee. 2017. Effect of full-span, artificial ice shapes on the performance of an 8.9% scale semispan swept wing. In: *9th AIAA Atmospheric and Space Environments Conference*. AIAA-2017-4373.

[27] Lum, C., N. Sandhu, J. Diebold, B. Woodard, and M. Bragg. 2017. The Application of a five-hole probe wake-survey technique to the study of swept wing icing aerodynamics," In: *9th AIAA Atmospheric and Space Environments Conference*. AIAA-2017-4374.

[28] Fujiwara, G., M. Bragg, S. Camello, and C. Lum. 2016. Computational and experimental ice accretions of large swept wings in the icing research tunnel. In: *8th AIAA Atmospheric and Space Environments Conference*. AIAA-2016-3734.

[29] Broeren, A., M. Potapczuk, S. Lee, A. Malone. B. Paul, Jr., and B. Woodard. 2016. Ice-Accretion test results for three large-scale swept-wing models in the NASA icing research tunnel. In: *8th AIAA Atmospheric and Space Environments Conference*. AIAA-2016-3733. NASA/TM—2016-219137.

[30] Fujiwara, G. and M. Bragg. 2017. 3D computational icing method for aircraft conceptual design. In: *9th AIAA Atmospheric and Space Environments Conference*. AIAA-2017-4375.